

Seismic response of masonry buildings with alternative techniques for in-plane strengthening of timber floors

Resposta sísmica de edifícios de alvenaria com pisos de madeira reforçados com técnicas alternativas

Roberto Scotta
Davide Trutalli
Luca Marchi
Luca Pozza
Michele Mirra

Abstract

In this work, the seismic behaviour of three case-study masonry buildings with traditional timber floors (simple layer of wooden boards) retrofitted with three alternative techniques has been analysed.

The modification of the seismic response of the buildings, depending on the type of the in-plane stiffening technique applied to the diaphragms, has been determined. The dynamic behaviour of the building has been analysed via non-linear dynamic analyses using three-dimensional finite element models. Hysteretic elements reproducing the actual non-linear behaviour of both masonry and floors have been calibrated according to experimental results from literature. For all the timber diaphragms, Incremental Dynamic Analyses were performed with seven seismic signals. Obtained results give important information on the modification of the seismic response of masonry buildings when alternative retrofitting methods of traditional timber floors are used.

Resumo

Neste trabalho é analisado o comportamento sísmico de três edifícios de alvenaria, cuja estrutura tradicional de piso em madeira (pavimento em tábuas de madeira simples) é reforçada com três técnicas alternativas.

Foi avaliada a alteração da resposta sísmica dos edifícios, em função do tipo de solução adotada na rigidificação dos diafragmas no seu plano. O comportamento dinâmico dos edifícios foi simulado recorrendo a análises dinâmicas não-lineares utilizando modelos tridimensionais de elementos finitos. Os modelos foram calibrados, com base em resultados experimentais disponíveis na literatura, incorporando elementos com comportamento não-linear histerético, quer para a alvenaria quer para os pisos. Para cada tipo de diafragma de madeira em estudo, foi realizada uma Análise Dinâmica Incremental (IDA) para sete sinais sísmicos. Os resultados obtidos fornecem informações importantes sobre a modificação da resposta sísmica dos edifícios de alvenaria quando são adotadas diferentes soluções de reforço ao nível dos seus pisos de madeira.

Keywords: Timber floors / Seismic behaviour / Strengthening techniques

Palavras-chave: Pavimentos em madeira / Comportamento sísmico / Técnicas de reforço

Roberto Scotta

MSc, PhD/Engineer
Department ICEA, University of Padova
Padova, Italy
roberto.scotta@dicea.unipd.it

Davide Trutalli

MSc, PhD/Engineer
Department ICEA, University of Padova
Padova, Italy
davide.trutalli@dicea.unipd.it

Luca Marchi

Msc, Phd Student/Engineer
Department ICEA, University of Padova
Padova, Italy
luca.marchi@dicea.unipd.it

Luca Pozza

MSc, PhD/Engineer
DICAM, University of Bologna
Bologna, Italy
luca.pozza2@unibo.it

Michele Mirra

MSc Student
Department ICEA, University of Padova
Padova, Italy
michele.mirra@studenti.unipd.it

Aviso legal

As opiniões manifestadas na Revista Portuguesa de Engenharia de Estruturas são da exclusiva responsabilidade dos seus autores.

Legal notice

The views expressed in the Portuguese Journal of Structural Engineering are the sole responsibility of the authors.

SCOTTA, Roberto [et al.] – Seismic response of masonry buildings with alternative techniques for in-plane strengthening of timber floors. **Revista Portuguesa de Engenharia de Estruturas**. Ed. LNEC. Série III. n.º 4. ISSN 2183-8488. (julho 2017) 47-58.

1 Introduction

Masonry buildings can be highly vulnerable to earthquake if in-plane strength and stiffness of floors are not sufficient to limit out-of-plane deformations of walls or portions of them or to transmit efficiently the seismic forces from floors to walls [1], [2].

Floors in masonry buildings, which are normally built with timber beams and a single orthogonal layer of timber boards nailed to the beams, lack of in-plane stiffness and strength is normally assumed as an improvement of the global seismic response of the building. Various strengthening techniques have been developed and can be applied as retrofitting methods: each one is characterized by a different efficiency, involving a not easily predictable response. Most common technologies and their details are summarized in [3], [4]. The RC slab connected to the existing timber beams with traditional or innovative anchorage techniques is the most widely used [5]-[7]. Another widely known method, which is a more compatible, lighter and reversible alternative, consists of the application of a second and sometimes a third layer of timber planks above the existing one, fastened to timber beams and arranged with an angle of 45° or 90°. Other methods consist of the application of timber panels (plywood, CLT, OSB...) fastened to the existing planks or the use of diagonal bracing system made with steel plates or FRP strips.

The in-plane stiffness of timber floors with different strengthening methods and their force-displacement behaviour have been studied by various researchers with tests (e.g., [4], [8], [9]) and numerical models have been performed to evaluate the seismic response of entire buildings (e.g., [10], [11]). However, some strengthening methodologies have recently demonstrated to be inadequate or, in some cases, unfavourable [4] and the effectiveness of such retrofitting techniques remains an open issue.

Various recent works have been carried out to evaluate the hysteretic behaviour of unreinforced masonry walls loaded in plane and out of plane (e.g., [12]-[14]) or to study the interaction between floors and masonry walls (e.g., [15]-[19]).

In this work, three case studies of two-storey masonry buildings have been analysed with three-dimensional numerical models to investigate the effects of the application of alternative retrofitting techniques to traditional timber floors (simple floor). The three considered retrofitting techniques are: a) addition of a second layer of timber boards fixed with screws to existing beams at an angle of 45°, b) use of light-gauge steel plates, c) usage of a lightweight reinforced concrete (RC) slab connected to the timber beams by means of studs. For each case-study building, results obtained for each technique are compared with those obtained with the original single-layer timber floor. A rigid connection of the timber floor with the surrounding masonry walls is assumed.

2 Numerical model of the building

The two-storey buildings have plan dimensions equal to 8.00 × 10.00 m and inter-storey height equal to 3.00 m. The first configuration (A) is regular in plan and in elevation, with four masonry piers parallel to the direction of the imposed seismic

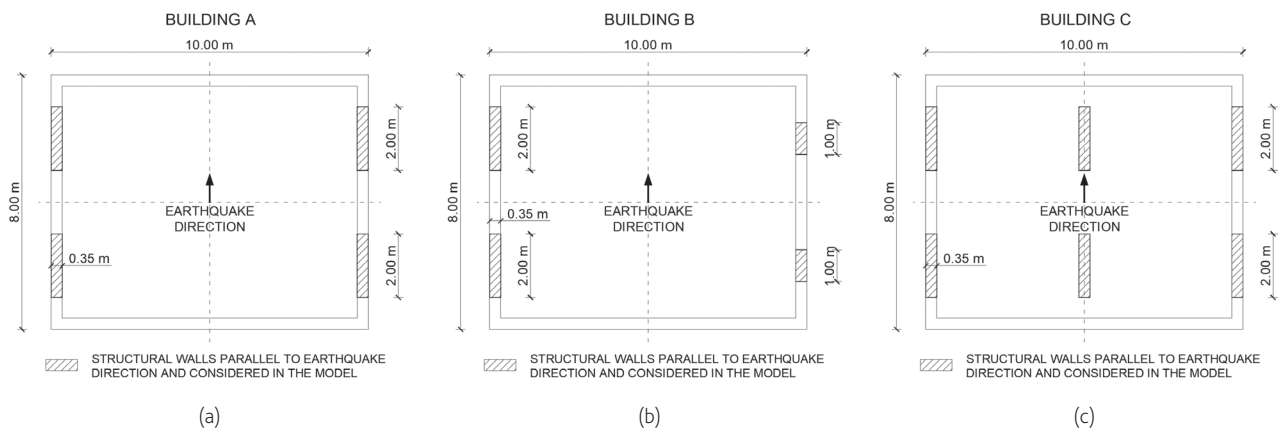


Figure 1 Building configurations: (a) regular (building A), (b) irregular (building B), (c) redundant (building C)

shocks, having base dimensions equal to 200×35 cm (Figure 1a) and aligned openings. The second configuration (B) is regular in elevation but not in plan. It has a geometry similar to A but walls in the east façade have base dimensions of 100×35 cm (Figure 1b). The last case study (C) is the same of A with two additional masonry piers in the middle of the floor span (Figure 1c). The latter configuration is characterized by the redundancy in the transmission of the horizontal loads among walls.

The details and mechanical parameters of the floors tested by Piazza *et al.* [4] and Baldessari [20] have been assumed. The not-strengthened floors (NS) are made with a single layer of 20×3 cm C22-class timber planks nailed orthogonally to 18×18 cm GL24c-class timber beams having spacing of 50 cm and fastened with 4 nails per intersection. The first strengthening technique (TB) consists of a second layer of 30-mm thick timber boards arranged at an angle of 45° to the first plank and fastened to the beams with 6×90 mm structural timber screws (from 2 to 4 screws per intersection). The second adopted method (SP) consists of the addition of light-gauge steel plates (80×2 mm) screwed to the existing boards at an angle of 45° with 5×25 mm screws (20 screws per meter). Spacing of diagonal bracing plates is 705 mm. The last chosen technique (RC) consists of the addition of a 50-mm thick RC slab reinforced with 6 mm diameter rebars (mesh 200×200 mm). Connection between timber beams and RC slab consists of 14 mm diameter L-shaped steel bars spaced 20-30 cm glued with epoxy resin.

In detail, twelve configurations have been analysed, which are labelled as follow (Table I):

- The first letter (A, B or C) identifies the wall configuration as described above;
- The second and third letter (NS, TB, SP or RC) identify the type of floor.

Masses and vertical loads have been computed according to the seismic combination of EN 1990 [21] assuming live loads equal to 2.00 kN/m^2 . Floor dead loads have been chosen according to the adopted strengthening technique including screed and finishing layers: they were assumed equal to 3.00 kN/m^2 for the NS, TB and SP configurations and 4.00 kN/m^2 for the RC ones. Masonry density was assumed equal to 18.00 kN/m^3 . Spread mass corresponding to

all non-structural walls and to structural walls orthogonal to seismic direction has been also considered in the numerical models and modelled as mass at floor levels. Conversely, their stiffening effects have been neglected, as they were not modelled.

Table I Case-study configurations

	Regular building	Irregular building	Redundant building
Existing floor with single layer of timber boards (simple floor)	A-NS	B-NS	C-NS
Existing floor reinforced with an additional timber layer at an angle of 45°	A-TB	B-TB	C-TB
Existing floor reinforced with additional light gauge steel plates at an angle of 45°	A-SP	B-SP	C-SP
Existing floor reinforced with additional 50 mm thick RC slab	A-RC	B-RC	C-RC

The numerical Finite-Element (FE) models for each building configuration were performed with the MidasGEN [22] software by assembling elements simulating masonry and floor behaviour (Figure 2). The main assumed modelling hypotheses are:

- Unreinforced masonry (URM) piers have a predominant rocking behaviour due to their dimensions and vertical load, therefore possibility of sliding and diagonal cracking failures has been neglected, so as the stiffening effects of spandrels;
- Masonry piers were modelled with non-linear beam elements having fibre section to simulate their hysteretic behaviour due to rocking;

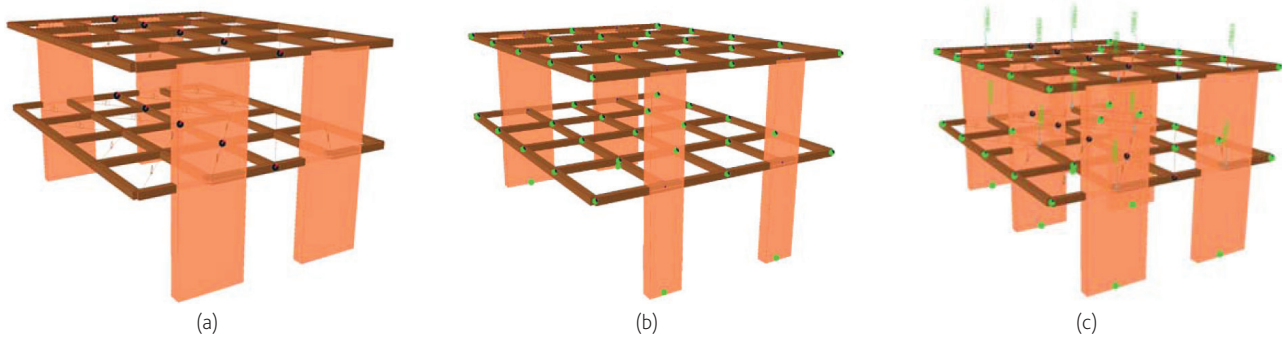


Figure 2 Axonometric views of the three-dimensional models: (a) building A, (b) building B, (c) building C

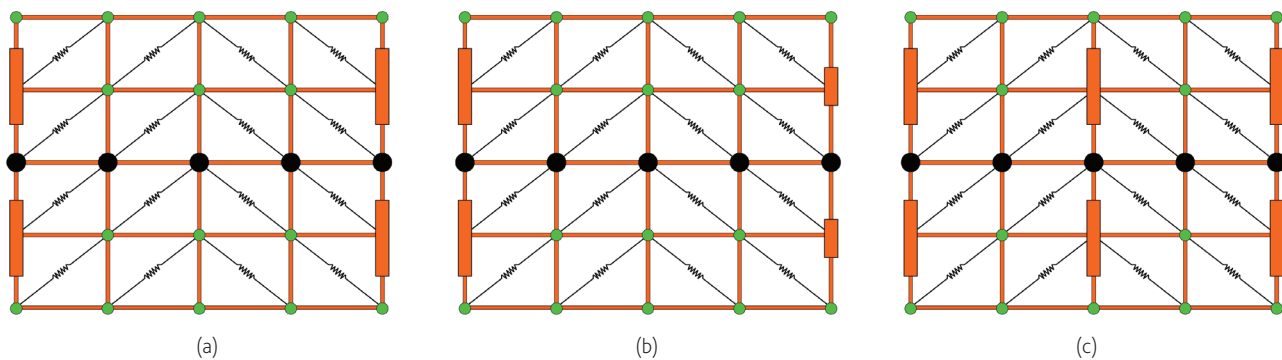


Figure 3 Plan views of the models: (a) building A, (b) building B, (c) building C

- The horizontal diaphragms were modelled as lattice modules composed of outer stiff elastic truss elements and non-linear springs as diagonals accounting for in-plane shear behaviour (Figure 3);
- All the masses have been modelled as translational point masses arranged in the floor nodes according to the relative pertinent areas (Figure 3). The masses of the structural walls parallel to the earthquake direction have been arranged at floor levels above walls. Conversely, the mass of the orthogonal walls is spread in all the floor nodes.

The feasibility of adopting a fibre beam model for masonry piers, notoriously unable of accounting for in-plane shear and diagonal cracking failures, was supported by preliminary analytical calculations. The maximum shear strength V_R of a single masonry pier and the equivalent bending moment M_R were analytically derived from [1] for each failure mode (i.e., rocking, sliding and diagonal cracking failure). Table II shows that, considering the actual dimensions and axial load acting on each masonry pier of the case-study buildings, rocking failure always anticipates other in-plane failures. Therefore, no more complex models are needed for piers.

Table II Shear strength and equivalent bending moments according to [1] for a single pier of $200 \times 35 \times 300$ cm, subjected to an axial load of 151.05 kN

Failure mode	Shear strength (kN)		Equivalent bending moment (kNm)	
	Parameter	Value	Parameter	Value
Rocking	V_R	41.83	M_R	125.49
Sliding	V_R	52.30	M_R	156.89
Diagonal cracking	V_R	77.42	M_R	232.25

2.1 Floor models

The hysteretic behaviour of all the diaphragms (NS, TB, SP, RC) was calibrated reproducing the quasi-static cyclic-loading tests conducted at University of Trento [20] according to EN 12512 [23]. The geometrical and mechanical characteristics of the diaphragms considered in this work are the same of the tested specimens. In particular, the Finite-Element (FE) model of the diaphragms was

obtained subdividing the original geometry of the tested floor module (plan dimensions 4.00×5.00 m) into four sub-modules 2.00×2.50 m, composed of stiff elastic truss elements at the perimeter and a single non-linear diagonal spring for each sub-module, as shown in Figure 4. The properties of trusses and diagonal springs were calibrated to reproduce the results from experimental tests [4]. The properties of trusses and diagonal springs were calibrated to reproduce the results from experimental tests [4]. To calibrate the floor models, elastic and post-elastic hardening stiffness and yielding point were obtained applying method "a" of EN 12512 [23] to the envelope curves of the experimental cycles. Then, cycles were fitted graphically and compared with experimental ones in terms of dissipated energy. Figure 5 shows the calibration of the in-plane shear behaviour of all analysed floors. It is worth noting that only the low displacement cycles from tests were considered for the calibration, i.e., within the displacement level consistent with the floor deformation of the case-study buildings conforming to masonry drift at failure, assumed equal to 0.8%.

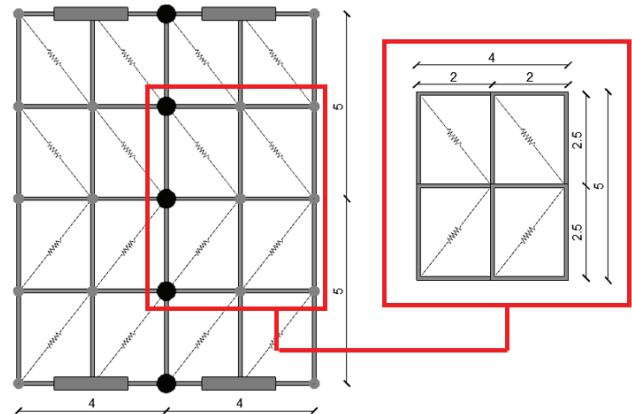


Figure 4 Modelling of the building diaphragms: subdivision of the 5×4 m module into sub-modules

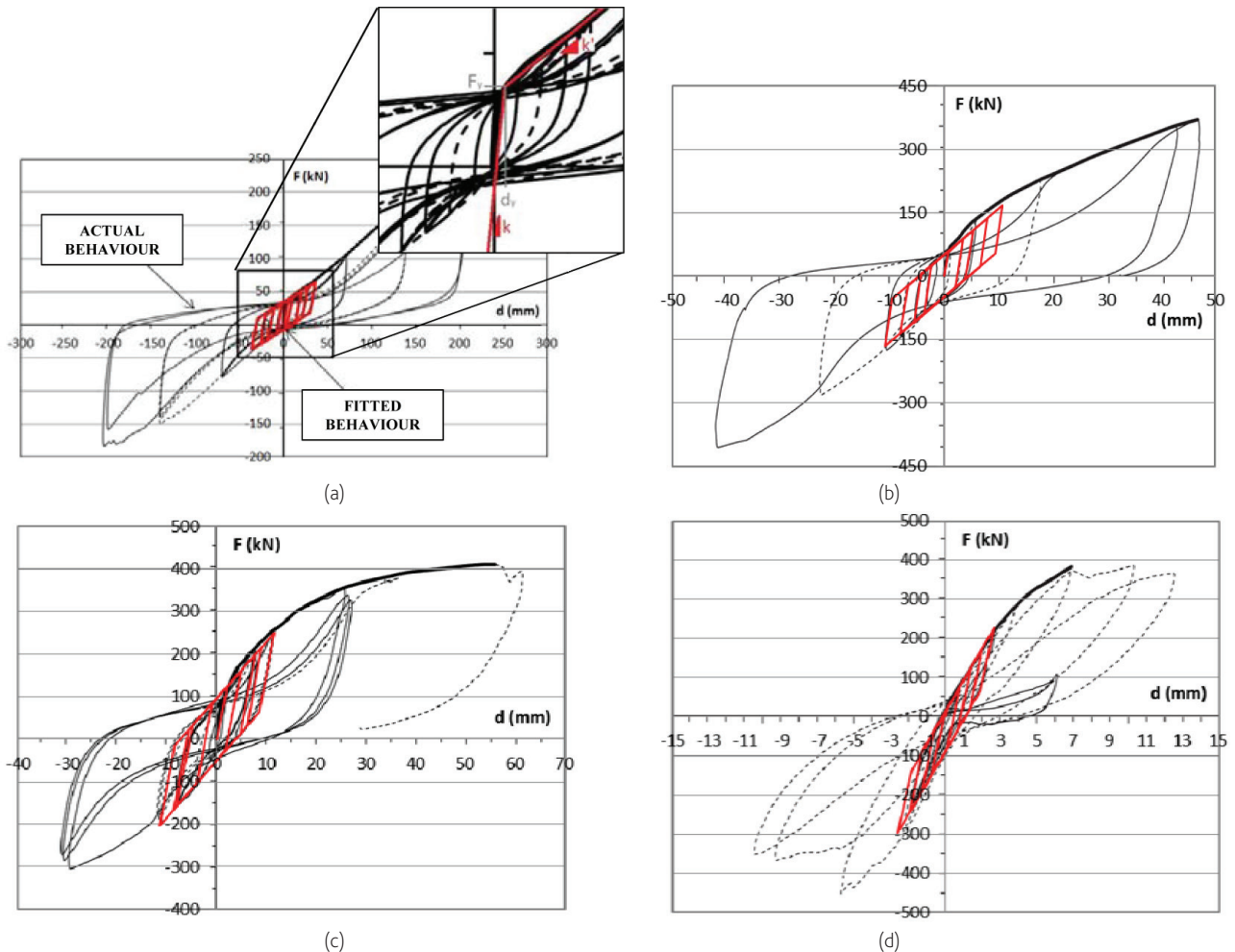


Figure 5 Calibration of diaphragms' models: total shear force vs. displacement measured at the mid span point for (a) NS floor; (b) TB floor; (c) SP floor; (d) RC floor

A first comparison among the considered strengthening methods can be made in terms of elastic stiffness k computed applying EN 12512 [23] (Table III). From these values, it is evident that all the strengthening methods strongly increase the stiffness of the simple floor (about 30 times for RC and on average 10 times for TB and SP).

Table III Comparison of elastic stiffness k among floors

	k (kN/mm)	k/k_{NS} (-)	k/k_{RC} (-)
NS	7.09	1.00	0.03
TB	80.00	11.28	0.35
SP	61.50	8.67	0.27
RC	230.00	32.44	1.00

2.2 Masonry model

A fibre beam model was chosen to simulate the actual hysteretic behaviour and failure of masonry piers due to rocking. A damage model was adopted to simulate the null tensile strength and brittle behaviour of masonry, allowing the possibility of representing cracking and compressive inelastic response, stiffness recovery at crack closure, softening branch and failure condition.

Kent and Park model [24], originally proposed to determine a stress-strain relation of concrete and implemented in MidasGEN library [22], was properly adapted to simulate the behaviour of masonry when subjected to compression loads. The mechanical parameters summarized in Table IV, which describe the skeleton curve, were calibrated from test available in literature [25] and represent the actual response of a masonry prism composed by typical clay bricks coupled with mortar.

Each beam element has the same cross-section of the actual masonry piers and length equal to the inter-storey height of the case-study building. Fibre's thickness was scaled according to the pier dimensions.

Table IV Mechanical parameters describing skeleton curve of Kent and Park model [24]

Parameter [Units]	Value	Skeleton curve
Elastic modulus [MPa]	E	2400.0
Shear modulus [MPa]	G	500.0
Compressive strength [MPa]	$f_{cd} = f_k$	3.0
Strain at maximum strength	ε_0	0.002
Strain at end of softening branch	ε_u	0.0036
Strain at failure	ε_1	0.004
Lateral confinement factor	k	1.0
Gradient of softening branch	Z	500.0

3 Numerical analyses and results

Preliminary non-linear static analyses (NLSA) were performed to determine the ultimate displacement capacity of masonry piers, necessary to define the in-plane failure conditions for the following non-linear dynamic analyses. A triangular distribution of equivalent seismic horizontal forces was applied to the structure and increasing monotonic displacements were imposed to the central node of the floors up to 70 mm at top floor, *i.e.*, up to the expected out-of-plane failure displacement of the wall orthogonal to the seismic input direction. Results of NLSA on building A are reported in Figure 6 where: dashed lines represent building base shear vs. displacement of the mid span point of first floor; continuous lines represent base shear of a single pier vs. displacements of the same pier (the base shear of the building is four times the base shear of the single pier). It can be seen that only for A-NS, displacement of floor differs from that of piers, whereas for all the strengthened floors (TB, SP, RC) mid-span floor and pier displacements are practically identical. This means that stiffness and strength of the strengthened floors are sufficient to transfer the same level of seismic force to the masonry piers, acting as almost rigid diaphragms in the considered building. The maximum in-plane displacement of piers measured at failure is about 24 mm, *i.e.*, corresponds to a drift of 0.8%, independently from the retrofitting technique.

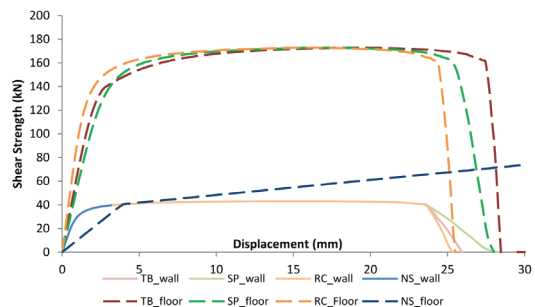
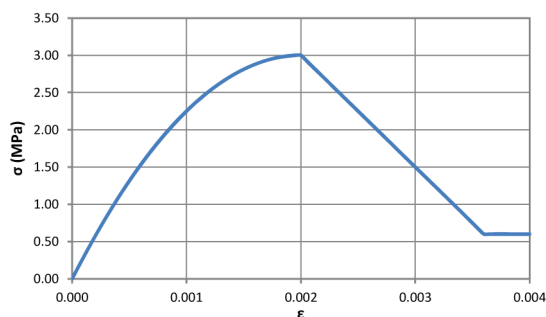


Figure 6 Capacity curves from pushover analyses for building A: effect of floor types



After NLSA, incremental dynamic analyses (IDA) with increasing Peak Ground Acceleration (PGA) level were performed for the evaluation of the near-collapse PGA, hereafter called PGA_u . A set of six artificial earthquakes [26] and one natural earthquake (El Centro) were applied to all models. The artificial earthquakes were generated respecting the spectrum compatibility requirements according to the elastic response spectrum for building foundations resting on type A soil (rock soil, corresponding to $S = 1.0$, $T_B = 0.15$ s, $T_C = 0.4$ s, $T_D = 2.0$ s) and building importance factor $\gamma_I = 1$, according to Eurocode 8 [27]. An estimation of the compatible elastic PGA (PGA_u) was computed via an equivalent linear static analysis (q-factor = 1.00) as the PGA which leads the masonry piers to rocking failure (i.e., to reach their ultimate resisting moment), considering the mass, the principal elastic period of the building and a spectral amplification factor $F_0 = 2.5$. From these calculations, it was obtained a PGA_u equal to 0.038 g, 0.015 g and 0.058 g for buildings A, B and C respectively with the original floors (NS cases).

Table V lists the main natural frequencies of all the buildings for each type of floor. Table VI gives the top displacement vs. base shear curves for each case study subjected to the same seismic signal. The other seismic signals gave similar results and led to the same conclusions. The cycles recorded at the middle node of the top floor (TF) are compared with the cycles of a masonry pier at the same level (MP). The comparison is given only between NS and TB floors, being results for SP and RC floors almost identical to the TB models. This evidence confirms that all the strengthening techniques have almost the same efficacy in limiting the in-plane deformation of floors, as demonstrated by the NLSA.

Table V Main natural vibration frequencies of each configuration (Values in Hz)

Floor Type	Building A	Building B	Building C
NS	2.50	1.18	3.23
TB / SP / RC	2.78	1.20	3.45

A first comparison between A-NS and A-TB buildings at low PGA allows a first interesting evidence: for the same low level of applied seismic inputs ($PGA = 0.077$ g), displacements and forces for A-TB are higher than A-NS. The level of PGA_u for which ultimate top displacement of piers is achieved resulted to be equal to 0.308 g for A-NS and 0.135 g for A-TB. Considering A-NS, the peak horizontal displacement of the floor is about 50% higher than that of the masonry wall. At PGA_u the out-of-plane displacement of non-structural walls remains limited to an acceptable value, and failure is achieved in the shear resisting walls, while for the A-TB case, hysteretic cycles of top floor and walls are identical evidencing the almost infinite stiffness of the retrofitted floors. The same displacements for all the piers have been noticed, independently from the stiffness of the floors.

In buildings B, failure is localized in the slender walls, whereas the 2.00 m walls remained almost elastic. The PGA_u were obviously lower than in building A: an uniform $PGA_u = 0.07$ g was obtained independently from the strengthening technique adopted for the

floors. This means that in building B even the NS floor is enough stiff and strong for the slender pier. The comparison between B-NS and B-TB in Table VI evidences that the strengthened floor induced higher displacement and forces than the 2.00 m wide walls.

In buildings C, the strengthened floors assure an equal displacement of the shear walls, while in C-NS the deformability of the floor allows for a slight higher displacement of the central wall. For the same level of PGA (as instance $PGA = 0.174$ g in Table VI) total displacement of the walls with the strengthened floor is again higher than with NS floor: PGA_u is equal to 0.29 g in the C-NS case, while it decreases in the range between 0.18 g and 0.24 g with the strengthened floors.

The above described results are in contrast with the widely accepted assumption that rigid floors can increase the seismic capacity of buildings. In all the three case-study buildings here considered, the retrofitting of timber floors caused a decrease of the seismic performance. In the following section, a discussion of the numerical results is conducted and the explanation of the reduced performance obtained with the retrofitted floors is given.

4 Discussion

The results from IDA presented in the previous section were averaged over seven seismic signals and analysed to draw conclusions about the effects of the floor stiffening.

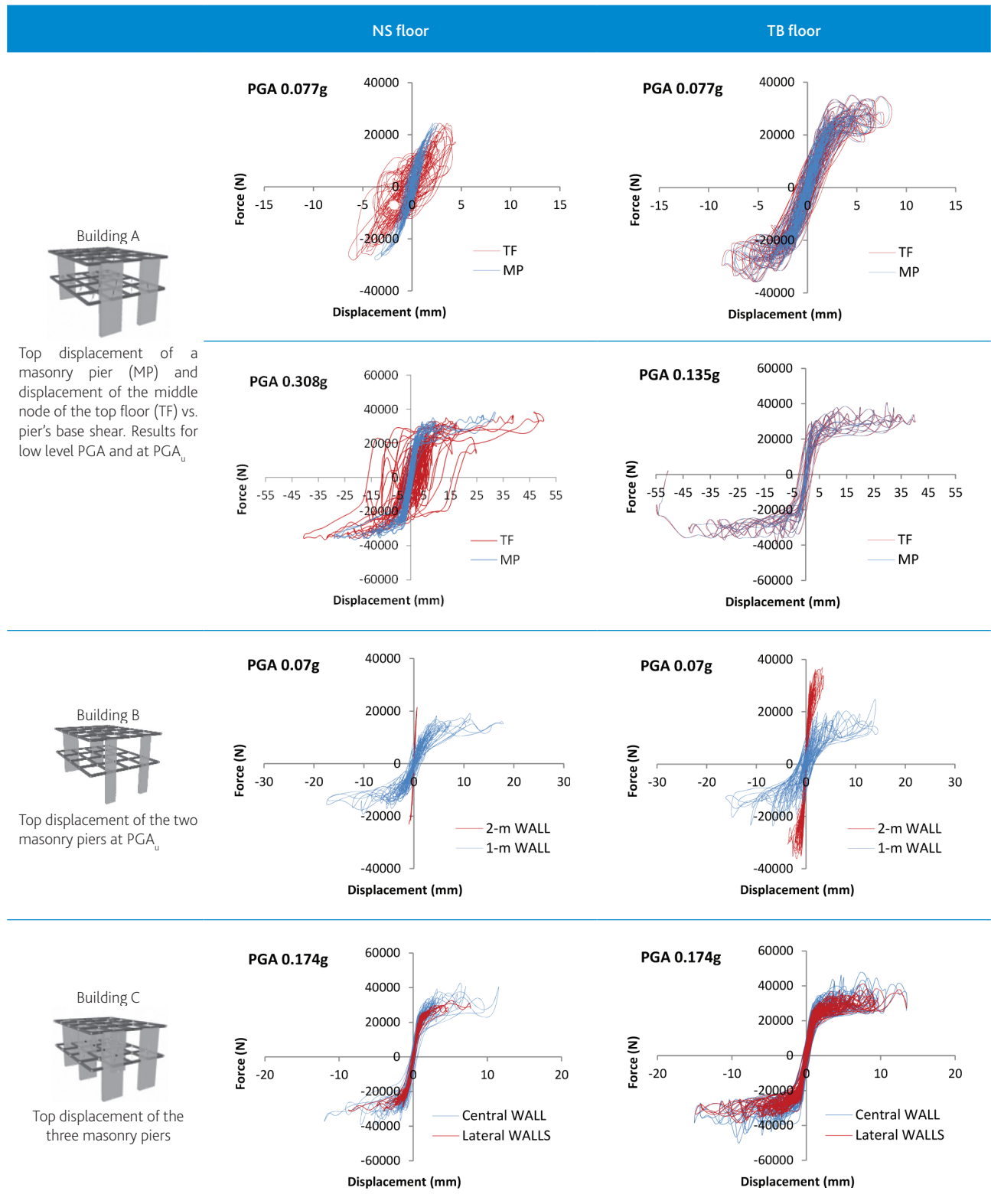
Figure 7 plots the trend of maximum horizontal displacement of mid-span floor and of walls recorded at the level of first floor with increasing PGA level. Displacements are averaged among the seven seismic signals.

As concerning building A, only the NS floor allows a significant difference between displacement of middle span point and of resisting walls (blue lines in Figure 7a), while all the lines of reinforced floors are superposed on those of walls, i.e., the floors are practically not deformable respect the walls and they remain in their elastic range. For a given value of PGA the displacements of the walls in the buildings with reinforced floors are always larger than in the A-NS case. Mean ultimate PGA value for which the displacement capacity of walls (24 mm) is exhausted is about 0.17 g in TB, SP and RC case. For NS, the mean PGA_u exceeds 0.3 g.

The motivation of such reduction of the seismic performance with retrofitting of floors has been found in the impaired dissipative capacity of the retrofitted floors. When stiffness of floors is increased, their capacity of energy dissipation is not exploited. Therefore, energy dissipation can be assured only by masonry piers with consequent increase of their mechanical damage. On the contrary, the NS floor is able to perform plastic deformations and to dissipate large amount of the energy inputted by the earthquake into the structure. NS floor acts as a damper, avoiding introduction of inertial loads into the shear walls. Consequently and contrarily to uniformly accepted design criteria, the interventions aiming to strengthen the floors may lead to a reduced overall dissipative capacity of the structure and to reduced seismic capacity.

Similar conclusion can be drawn analysing the numerical results obtained for building C. Such case study demonstrates also that the deformability of NS floors is not negligible but stiffness is enough

Table VI Comparison of results from IDA for a given seismic signal



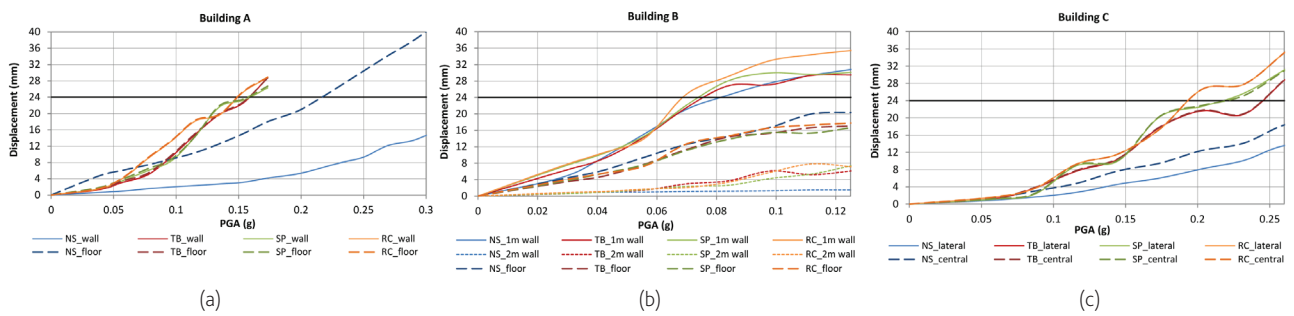


Figure 7 Mean maximum displacements of floor and walls from IDA at first floor level vs. imposed PGA. (a) Building A: wall and floor. (b) Building B: 1.0 m wall, 2.0 m wall and floor. (c) Building C: lateral wall and central wall

to assure a quite good distribution of seismic forces on the resisting shear walls. Figure 7c shows that with NS floors, mean displacement of lateral walls (continuous blue line) is about 80% of that of central wall (dashed blue line). With the retrofitted floors, relative displacements of the shear walls are zeroed, *i.e.*, rigid translation of the floors occurs. Even in building C adoption of rigid, and then non-dissipating, floors leads to increased displacement and to reduced PGA_u .

Case study B is less significant, being the NS floor stronger and stiffer than the weak 1.0 m wide shear wall. In this case, alternative

options for floors do not affect significantly their mean maximum displacements, which are intermediate between the displacements of the 2.0 m wall and of the 1.0 m wall.

Consideration about relevance of energy dissipation from floor distortion has been evidenced by computing the energy dissipated by floors and walls as a fraction of the input seismic energy. Results are plotted in Figure 8 where, for the same seismic input, time evolution of inputted and dissipated energies are reported for case study A and the various floor options. The dissipated energies are computed as the area within hysteretic cycles of floors and walls. The

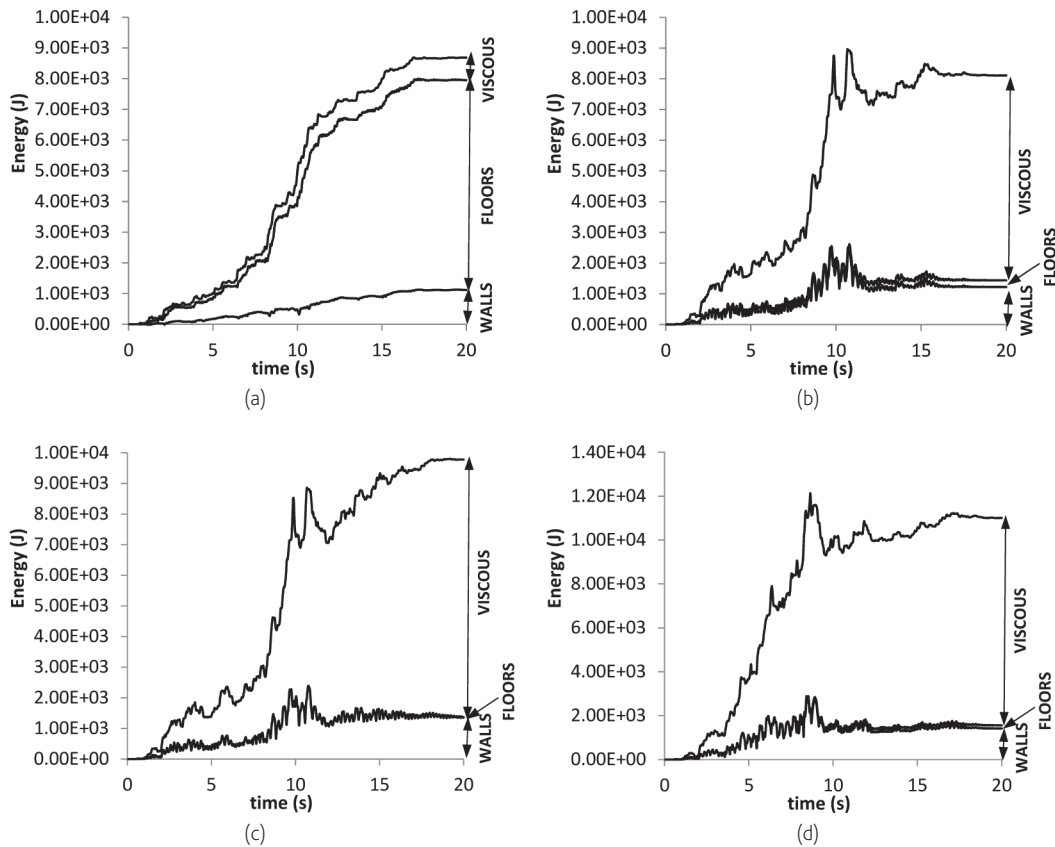


Figure 8 Energetic response for Building A for a typical seismic signal: (a) A-NS; (b) A-TB; (c) A-SP; (d) A-RC

inputted energy is the work done by seismic input on the structure as a whole, computed according to [28]. The gap between inputted energy and summation of dissipated energies gives the viscous energy contribution (in the numerical models a 2% Rayleigh viscous damping has been considered), which is emphasized for buildings having an almost elastic behaviour.

Obtained results confirm that in A-NS building floors dissipated most of the inputted energy, transmitting to walls reduced seismic forces. Conversely, for all the retrofitted buildings, floors showed a negligible dissipative contribution, independently from the chosen retrofitting strategy. Therefore, it can be stated that for these buildings seismic forces derived from dead and live masses of floors are totally transferred to the shear walls.

The aforementioned results can be useful to provide additional information to design properly such structural rehabilitations. When performing linear analyses, normally strengthened floors are schematized as infinitely rigid in their plane and the different dissipative capacity provided by the type of floor adopted is not taken into account. According to results presented in this work, it seems appropriate to consider different values of the equivalent viscous damping ξ [27] in linear numerical models to take into account the different dissipative capacity supplied by the floor deformation. A first estimation of these values has been obtained for Building A performing additional analyses at PGA_u for each case study, modelling all floors with pure elastic behaviour and increasing the value of ξ in the model until reaching the masonry failure deformation. The estimations of ξ are listed in Table VII.

Table VII Evaluation of viscous damping ξ for building A

	PGA_e (g)	PGA_u (g)	ξ (-)
NS	0.038	0.308	7.50
TB	0.038	0.135	5.50
SP	0.038	0.135	5.50
RC	0.038	0.135	2.00

5 Conclusions

Results presented in this work were obtained from numerical analyses performed to simulate the non-linear behaviour of masonry buildings with simple or strengthened timber floors. Such models have been used to estimate how the seismic response of different masonry case-study buildings is modified by different rehabilitation techniques of the timber floors.

The main hypotheses and simplifications assumed in this work, from which results are conditioned, are:

- A rigid anchorage of the diaphragms to perimeter walls has been assumed;
- The structural walls orthogonal to the seismic direction have not been modelled, therefore their possible stiffening effects have been neglected;
- The mass of the structural walls orthogonal to the seismic

direction has been arranged in the floor nodes;

- The possible stiffening effects of screeds have been neglected, thus assuming the presence of screeds with loose materials.

From the numerical results and considering the aforementioned hypotheses, some conclusions and some useful information for the design may be obtained:

- It is necessary to find a correct ratio between the increase of in-plane stiffness of the floor (necessary to transmit correctly the forces to the walls) and the decrease of its dissipative capacity;
- The use of a 45° additional layer of timber boards fastened with screws, of light-gauge steel plates or of a 50 mm RC slab gives almost the same in-plane response of the floor. These diaphragms can be properly considered as infinitely stiff in their plane and modelled accordingly;
- In contrast to common expectations, the seismic capacity of a traditional masonry building can decrease if a retrofitting method leading to excessive floor stiffening is adopted.

This last conclusion derives from results in terms of PGA: the analysed retrofitted buildings have withstood earthquakes with lower intensities than un-reinforced ones, *i.e.*, all the applied retrofitting strategies have worsened the seismic performances. This suggests therefore that interventions aiming to stiffen the floors can impair the seismic response of a structure affecting its displacement and dissipative capacity. Conversely, a deformable floor can act as a dissipative damper interposed between the floor mass and the resisting shear walls, if it is characterized by a dissipative non-linear behaviour after yielding. The dissipation capacity and the possible increasing of the oscillation period, if it is higher than the upper limit of the constant spectral acceleration branch of the spectrum (plateau), produce a reduction of seismic forces on resisting walls.

Further works are needed to generalize the results considering other case-study buildings and in particular more refined three-dimensional models, which consider the behaviour of the walls perpendicular to the earthquake direction and other possible in-plane failure modes of masonry, *i.e.*, sliding or diagonal cracking.

Acknowledgments

The authors acknowledge the contribution to the research given by Luca De Tomasi and Andrea Lonardi with the development of their master theses.

References

- [1] Magenes, G.; Calvi, G.M. – “In-plane seismic response of brick masonry walls”. *Earthquake Engineering and Structural Dynamics*, 26, 1091-1112, 1997.
- [2] Giuriani, E.; Marini, A. – “Wooden roof box structure for the anti-seismic strengthening of historic buildings”. *International Journal of Architectural Heritage*, 2(3), 226-246, 2008.
- [3] Ongaretto *et al.* – “Wood-based solutions to improve quality and safety against seismic events in conservation of historical buildings”. *International Journal for Quality Research*, 10(1), 17-46, 2016 doi: 10.18421/IJQR10.01-01.

- [4] Piazza *et al.* – “The role of in-plane floor stiffness in the seismic behaviour of traditional buildings”. 14th World Conference on Earthquake Engineering, Beijing, China, 2008.
- [5] Piazza, M.; Turrini, G. – “Una tecnica di recupero statico dei solai in legno”. *Recuperare*, 5, 224-237, Milano, 1983.
- [6] Crocetti *et al.* – “An innovative prefabricated timber-concrete composite system”. *Materials and Joints in Timber Structures*, 9, 507-516, 2014.
- [7] Marchi *et al.* – “Experimental and theoretical evaluation of TCC connections with inclined self-tapping screws”. *Materials and Structures*. 2017 doi: 10.1617/s11527-017-1047-1.
- [8] Newcombe *et al.* – “In-Plane Experimental Testing of Timber-Concrete Composite Floor Diaphragms”. *Journal of Structural Engineering*, ASCE, 136(11), 1461-1468, 2010.
- [9] Valluzzi *et al.* – “In-plane strengthening of timber floors for the seismic improvement of masonry buildings”. *Proceedings of the World Conference on Timber Engineering WCTE*, Riva del Garda, Italy, 2010.
- [10] Brignola, A. *et al.* – “In-plane stiffness of wooden floor”, NZSEE Conference, Wairakei, New Zealand, 2008.
- [11] Gattesco *et al.* – “Retrofit of wooden floors for the seismic adjustment of historical buildings with high reversible techniques”. ANIDIS, Pisa, Italy, 2007.
- [12] Beyer, K. – “Peak and residual strength of brick masonry spandrels”. *Engineering Structures*, 41, 533-547, 2012.
- [13] Allen *et al.* – “Cyclic in-plane shear testing of unreinforced masonry walls with openings”. *Proceedings of the Tenth Pacific Conference on Earthquake Engineering*, Sydney, Australia, 2015.
- [14] Vaculik, J.; Griffith, M. – “Shaketable Tests on Masonry Walls in Two-Way Bending”. Australian Earthquake Engineering Society Conference, Wollongong, NSW, Australia, 2007.
- [15] Tondelli *et al.* – “Influence of boundary conditions on the out-of-plane response of brick masonry walls in buildings with RC slabs”. *Earthquake Engng Struct. Dyn.*, 45(8), 1337-1356, 2016.
- [16] Giongo I *et al.* – “Field Testing of Flexible Timber Diaphragms in an Existing Vintage URM Building”. *Journal of Structural Engineering*, 2015, DOI: 10.1061/(ASCE)ST.1943-541X.0001045.
- [17] Costley, A.C.; Abrams, D.P. – “Dynamic response of unreinforced masonry buildings with flexible diaphragms”. National Center for Earthquake Engineering Research, 1996.
- [18] Simsir *et al.* – “Out-of-plane dynamic response of unreinforced masonry bearing walls attached to flexible diaphragms”. 13th WCEE, Vancouver, B.C., Canada, 2004.
- [19] Paquette, J.; Bruneau M. – “Pseudo-Dynamic Testing of Unreinforced Masonry Building with Flexible Diaphragm”. *Journal of Structural Engineering*, 129(6), 708-716, 2003.
- [20] Baldessari, C. – *In-plane behaviour of differently refurbished timber floors*. Ph.D Thesis, University of Trento, Italy, 2010.
- [21] EN 1990 “Eurocode - Basis of structural design”, European Committee for Standardization (CEN), 2010.
- [22] MIDAS/Gen FX Program. MIDAS/Gen FX – General structure design system. <http://www.cpsfea.net>.
- [23] EN 12512 – “Timber structures – test methods – cyclic testing of joints made with mechanical fasteners”. European Committee for Standardization (CEN), 2006.
- [24] Kent, D.C.; Park, R. – “Flexural members with confined concrete”, *Journal of the Structural Division*, 97, 1969-1990, 1971.
- [25] Kaushik *et al.* – “Stress-strain characteristics of clay brick masonry under uniaxial compression”, *Journal of materials in Civil Engineering*, 19(9), 728-739, 2007.
- [26] Gelfi, P. (2012) – SIMQKE_GR, Version 2.7. University of Brescia, Italy. Available online: <http://dicata.ing.unibs.it/gelfi>.
- [27] EN 1998-1 – “Eurocode 8: design of structures for earthquake resistance, part 1: General rules, seismic actions and rules for buildings”. European Committee for Standardization (CEN), 2013.
- [28] Uang, C.M.; Bertero, V. – “Evaluation of seismic energy in structures”. *Earthquake engineering and structural dynamics*, 19, 77-90, 1990.

